Negative correlation between charge carrier density and mobility fluctuations in graphene

Jianming Lu,[1,*] Jie Pan,[1,*] Sheng-Shiuan Yeh,[2] Haijing Zhang,[1] Yuan Zheng,[1] Qihong Chen,[1]
Zhe Wang,[1] Bing Zhang,[1] Juhn-Jong Lin,[2] and Ping Sheng[1,3,†]
[1]*Department of Physics and William Mong Institute of Nano Science and Technology, Hong Kong University of Science and Technology, Clear Water Bay, Kowloon, Hong Kong, China*
[2]*Institute of Physics and Department of Electrophysics, National Chiao Tung University, Hsinchu 30010, Taiwan*
[3]*Institute for Advanced Study, Hong Kong University of Science and Technology, Clear Water Bay, Kowloon, Hong Kong, China*
(Received 4 November 2013; revised manuscript received 26 June 2014; published 26 August 2014)

By carrying out simultaneous longitudinal and Hall measurements in graphene, we find that the $1/f$ noise for the charge carrier density is negatively correlated to that of mobility, with a governing behavior that differs significantly from the relation between their mean values. The correlation in the noise data can be quantitatively explained by a single-parameter theory whose underlying physics is the trapping and detrapping of the fluctuating charge carriers by the oppositely charged Coulomb scattering centers. This can alter the effective density of long-range scattering centers in a transient manner, with the consequent fluctuating effect on the mobility.

DOI: 10.1103/PhysRevB.90.085434 PACS number(s): 72.70.+m, 72.10.Fk, 72.80.Vp, 73.20.Hb

I. INTRODUCTION

Flicker noise, also denoted the $1/f$ noise, has been a subject of extensive investigations for almost one century [1]. However, the debate about its origin and underlying physical mechanisms still persists. With the recent advent of graphene and its various potential applications, such as field-effect transistors (FETs) [2], magnetic field sensors [3–5], and gas molecular or even biomolecular sensors [6–8], flicker noise has attracted renewed attention as an important factor that can affect device performance. In particular, mobility fluctuations and their relation to changing configurations of charged impurities in graphene have been raised [9]. It was proposed [10] that the fluctuating and static components of resistance can arise from different scattering mechanisms, i.e., short- or long-range scatterings. The gate voltage dependence of the flicker noise was also interpreted as arising from mobility fluctuations, owing to both short-range (defect configuration) and long-range (Coulomb) scatterings [11].

In spite of the extensive literature on flicker noise in graphene [9–27], the microscopic reasons why mobility fluctuations play a dominant role are still barely understood. A definitive picture of correlation between the carrier density fluctuations and mobility fluctuations would contribute to our understanding of the underlying mechanisms. In this paper, we present a straightforward approach to simultaneously obtain carrier density fluctuations as well as the mobility fluctuations, by measuring the Hall voltage and the longitudinal resistance at the same time and on the same area of a sample. The results show that not only the Hall voltage fluctuations and the longitudinal voltage fluctuations are nearly uncorrelated, but also the mobility and charge carrier density fluctuations are negatively correlated. Such results differ dramatically from semiconducting systems [28].

In our experiments, the measured quantities are the longitudinal voltage $V_{xx} = I/\sigma$ and Hall voltage $V_H = IB/ne$, both as a function of time. Here I denotes current, B denotes the applied magnetic field perpendicular to the sample, σ is longitudinal conductance, n is the charge carrier density, and e is the electronic charge. It follows that for an Ohmic system, the fluctuations in the two measured quantities, relative to their mean values, can be expressed as $\delta V_{xx}/V_{xx} = -\delta\sigma/\sigma$ and $\delta V_H/V_H = -\delta n/n$, where the fluctuation δQ of a physical quantity Q is defined as $\delta Q = Q(t) - \langle Q\rangle$, with $\langle Q\rangle$ denoting the time-averaged value. Thus one can unambiguously obtain the charge carrier density fluctuations δn directly from the Hall voltage measurements, unaffected by mobility fluctuations [29–31]. Since $\sigma = ne\mu$, where μ denotes mobility, we have $\delta\sigma = e\mu\delta n + en\delta\mu$, so that the fluctuation power integrated over the whole area may be expressed as $\langle(\delta\sigma/\sigma)^2\rangle = \langle(\delta n/n)^2\rangle + \langle(\delta\mu/\mu)^2\rangle + 2\langle(\delta n/n)(\delta\mu/\mu)\rangle$. Here the angular brackets denote time averaging or ensemble averaging, or both. Measurement over the same area of the sample is assumed in the above. The last term on the right-hand side is the correlation term between $\delta n/n$ and $\delta\mu/\mu$. If $\delta n/n$ and $\delta\mu/\mu$ are independent, then $\langle(\delta n/n)(\delta\mu/\mu)\rangle = 0$ and the longitudinal resistance and/or conductance fluctuations $\langle(\delta\sigma/\sigma)^2\rangle$ should have a larger magnitude than that of the Hall voltage, which depends only on the charge carrier density $\langle(\delta n/n)^2\rangle$.

Our first observation is that we have consistently observed in multiple graphene samples that the normalized Hall noise, i.e., the carrier density noise, can exceed the longitudinal noise. This is only possible if the fluctuations of the charge carrier density and mobility are negatively correlated, i.e., $\langle(\delta n/n)(\delta\mu/\mu)\rangle < 0$. That is, the observation of $\gamma_H \equiv (S_{VH}/V_H^2)/(S_{V_{xx}}/V_{xx}^2) > 1$ gives support to negatively correlated mobility fluctuations with charge carrier fluctuations, arising from their trapping-detrapping process [32] by the Coulomb trapping centers. This can occur when the charge carriers have a different sign from the charged trapping centers [33]. Here S_{VH} and $S_{V_{xx}}$ denote Hall and longitudinal voltage noise power spectrum density (PSD), respectively. It should be noted that $S_{V_{xx}}/V_{xx}^2 \propto \langle\delta\rho^2\rangle/\rho^2 = \langle\delta\sigma^2\rangle/\sigma^2$, where $\rho = 1/\sigma$ denotes resistivity, and $\langle\delta\sigma^2\rangle$, $\langle\delta\rho^2\rangle$ the variance of the measured quantities.

A second observation is that the longitudinal resistance fluctuations are not correlated with the Hall voltage fluctuations. This is in contrast to the strong correlation between

*These two authors contributed equally to this work.
†sheng@ust.hk

 ©2014 American Physical Society

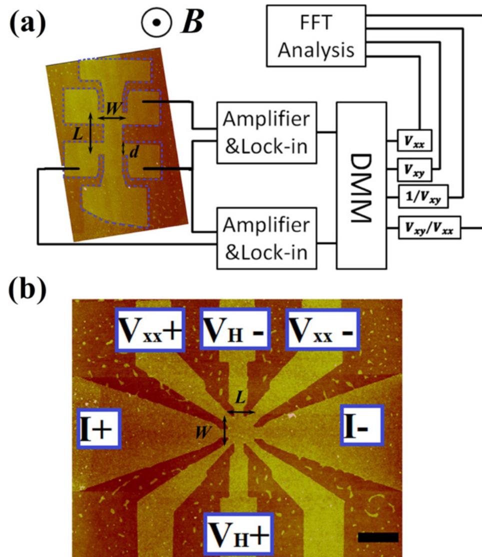

FIG. 1. (Color online) (a) Graphene flake of sample A is measured in perpendicular magnetic field under various temperatures. Longitudinal voltage (V_{xx}) and Hall voltage (V_H) are collected simultaneously and subsequently analyzed. Sample A is etched into the standard Hall-bar geometry, shown in the inset by the atomic force microscope (AFM) image. The geometric parameters are $L = 1.6\ \mu$m, $W = 1.2\ \mu$m, and $d = 0.4\ \mu$m. (b) Sample B in square (cross-bar) geometry is imaged by AFM. The scale bar on the lower right is 1 μm. Measurement probes are labeled as shown. Sample B's geometric parameters are $L = W = 0.6\ \mu$m.

longitudinal resistance fluctuations and Hall voltage fluctuations observed in semiconductors [28], since both quantities contain charge carrier density n. The near absence of correlation in our graphene samples indicates that the source of longitudinal fluctuations can be attributed to pure mobility fluctuations. This work intends to show that there is a simple explanation which can reconcile the above two observations.

In what follows, the experimental details are described in Sec. II, and the measurement results, on both the time-averaged behavior and fluctuations, are presented in Sec. III. In Sec. IV we give a consistent physical interpretation to our noise correlation results, based on the mechanism of trapping and detrapping of the charge carriers by the Coulomb impurities. A one-parameter theory is shown to give an excellent quantitative account of all the observations. We conclude in Sec. V by summarizing the few essential points deduced from the theory and experiment of this work, and pointing out some of the implications.

II. MEASUREMENT SETUP

Figure 1(a) shows the setup for the simultaneous measurements of V_{xx} and V_H in a perpendicular magnetic field. Exfoliated graphene flakes were patterned into two types of geometry, sample A in standard Hall-bar geometry ($L = 1.6\ \mu$m, $W = 1.2\ \mu$m) and sample B in the square, cross-bar geometry ($L = W = 0.6\ \mu$m), as shown in Figs. 1(a) and 1(b). Ti/Au electrodes were deposited with *e*-beam evaporation. After being transferred into the Physical Properties Measurement System (Quantum Design) with *in situ* baking at 400 K for 2 h, the noise measurement was conducted with ac current from lock-in SR850 output in series with a ballast resistor (10 MΩ) at $f = 1237$ Hz, so as to minimize the $1/f$ noise from the preamplifier SR560. Signals were simultaneously collected in the buffers of two lock-in amplifiers, then sent to a computer for analysis.

From $V_{xx}(t)$ and $V_H(t)$, simple mathematical operations lead to $n(t) = IB/eV_H(t)$ and $\mu(t) = V_H(t)/[V_{xx}(t)B]$. From the four time series one can easily obtain the four respective power spectrum densities (PSDs): $S_{V_{xx}}$, S_{VH}, S_n, and S_μ. Note that in graphene, Hall mobility is equivalent to the effective mobility [34,35], so we use the term "mobility" in what follows. For the convenience of the following discussion of our experimental results, we list here the relevant relations for the PSDs: $\frac{S_{V_{xx}}}{V_{xx}^2} \propto \frac{\langle\delta\sigma^2\rangle}{\sigma^2} = \frac{\langle\delta\rho^2\rangle}{\rho^2}$, $\frac{S_{V_H}}{V_H^2} = \frac{S_n}{n^2} \propto \frac{\langle\delta n^2\rangle}{n^2}$, and $\frac{S_\mu}{\mu^2} \propto \frac{\langle\delta\mu^2\rangle}{\mu^2}$. These relations can be easily derived from $\delta V_{xx}/V_{xx} = -\delta\sigma/\sigma$ and $\delta V_H/V_H = -\delta n/n$.

III. EXPERIMENTAL RESULTS

We will first show our samples' equilibrium (time-averaged) characteristics, followed by the presentation of the measured noise. We focus on the comparison between the normalized noise magnitudes of longitudinal and Hall voltages. Our results clearly indicate a negative correlation between the mobility and carrier density fluctuations $\langle(\delta n/n)(\delta\mu/\mu)\rangle < 0$, true for both samples A and B.

A. Sample characterization

The equilibrium (time-averaged) characteristics of sample A are shown in Fig. 2. At 150 K, the measured longitudinal resistances under $B = 0$ (black circles) and

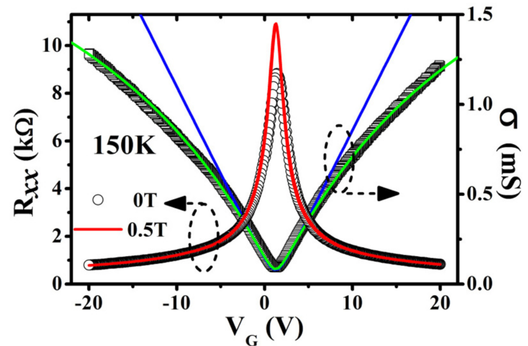

FIG. 2. (Color online) Longitudinal resistance, measured as a function of back gate voltage at 150 K, is shown on the left axis for $B = 0$ (black circles), 0.5 T (red line). The coincidence of the resistances measured under two different magnetic fields, in the region away from the charge neutral point, indicates the absence of quantum correction of longitudinal resistance at low magnetic field. Conductance at 0.5 T is plotted with black squares (scale is shown on the right) together with the green fitting curve that accounts for the long- and short-range scatterings. The deviation at $|V_G - V_{\rm CNP}| > 5$ V from the blue reference curve (only long-range scatterings) indicates the importance of the short-range scattering mechanisms. Data are from sample A.

$B = 0.5$ T (red line) are seen to display no difference at $|V_G - V_{\rm CNP}| > 4$ V, i.e., $\Delta\rho_{xx} = \rho(B) - \rho(0) \simeq 0$. Hence $\rho_{xy} \propto 1/ne$ since the correction term to this relation is proportional to $\Delta\rho_{xx}$. Conductance σ at $B = 0.5$ T (black square) is well fitted by [36] $\sigma = [\rho_S + (e\mu_0\sqrt{N^2 + n_0^2})^{-1}]^{-1}$, where the resistivity due to short-range scattering $\rho_s = 330\ \Omega$, and impurity- or inhomogeneities-induced carrier density $N = 0.6 \times 10^{11}$ cm^{-2}. The subscript zero indicates the quantities to be time-averaged values, to be distinguished from the instantaneous values that are the basis of noise measurements. The small magnitude of N indicates the graphene sample to be fairly pristine, while the relatively large value of ρ_s implies that the short-range scatterings play an important role in electron transport. As a reference, the blue curve is for no short-range scatterings, i.e., $\rho_s = 0$.

In graphene, it is well known that there can be puddles of positive and negative charge carriers arising from the gentle substrate undulations. The charge carriers arising from these puddles can play an important role for the graphene characteristics close to the charge neutrality point (CNP). To avoid the complications arising from the simultaneous existence of charge carriers of both signs, in this work we focus on the gate voltage in the range of $|V_G - V_{\rm CNP}| > 4$ V, in which $n(t)$ and $\mu(t)$ can be accurately deduced from $V_H(t)$ and $V_{xx}(t)$. This is supported by the linear behavior of deduced n with respect to V_G [Fig. 4(b)]. In contrast, for $|V_G - V_{\rm CNP}| < 4$ V the appearance of a small amount of magnetoresistance, probably due to the electron-hole puddle [37], complicates the physical picture. Hence in what follows the condition $|V_G - V_{\rm CNP}| > 4$ V is assumed unless otherwise specified.

B. Current dependence of $1/f$ noise

To check the dependence of $1/f$ noise on applied current, we use sample B [square cross-bar geometry as shown in Fig. 1(b)] to measure the magnitude of $1/f$ noise with different applied current levels, varying from 0.05 to 0.4 μA. For each current level, the PSDs for the longitudinal and Hall noise are plotted in Figs. 3(a) and 3(b), respectively. To exclude spurious noise peaks above 10 Hz, a low-pass filter in a lock-in amplifier was implemented with a cutoff frequency of 2.6 Hz. In practice, only the low-frequency part was used to evaluate the noise magnitude. In addition, noise background (black curve) was also measured and found to be smaller than the flicker noise by more than one order of magnitude.

The current dependence of the flicker noise is shown in Fig. 3(c) in log-log scale for both the longitudinal noise (filled symbols) and Hall noise (open symbols). Shown in Figs. 3(a) and 3(b) are the noise spectra for $V_G - V_{\rm CNP} = -36$ V and $V_G - V_{\rm CNP} = -16$ V. All the curves have a slope of 2, indicating the magnitude of the noise is proportional to the square of the current, demonstrating that the observed low-frequency noise in longitudinal and transverse directions originated from longitudinal resistance fluctuations and Hall-voltage fluctuations, respectively, in our graphene samples. It also indicates that the background noise is small enough to be neglected.

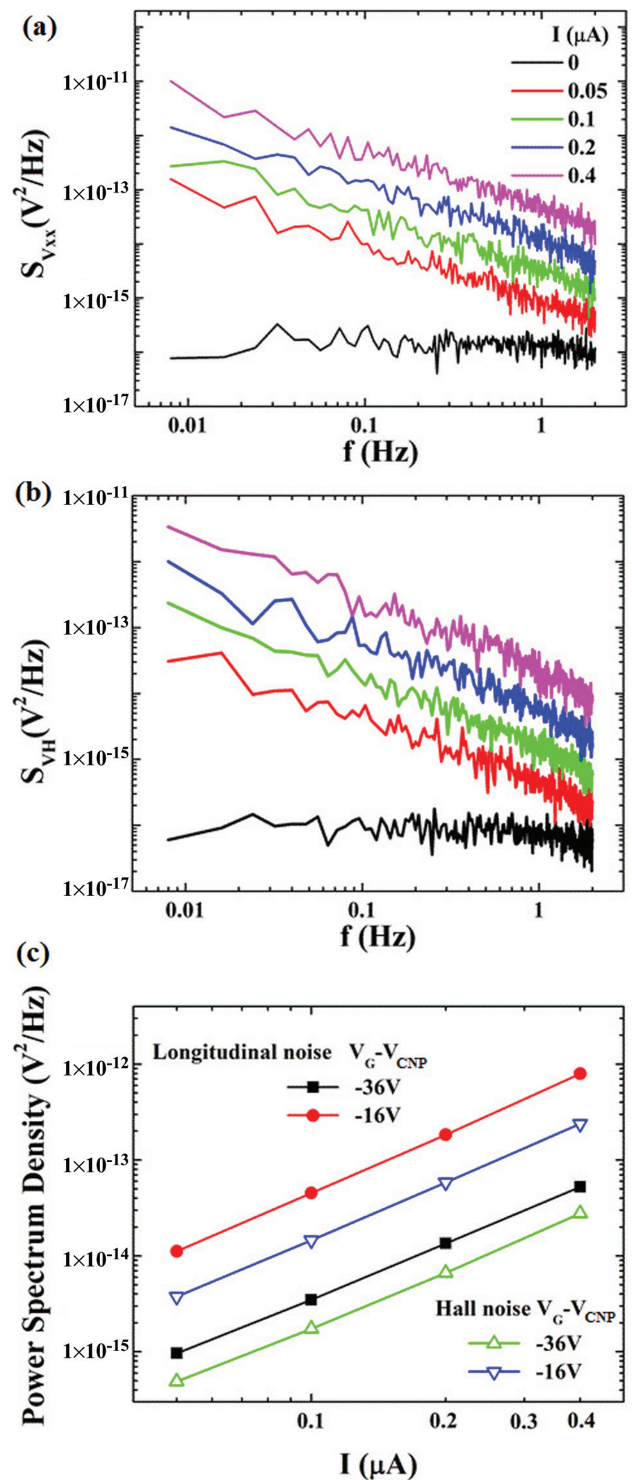

FIG. 3. (Color online) (a) Power spectrum density of longitudinal noise with current levels varying from zero to 0.05, 0.1, 0.2, and 0.4 μA are shown for $V_G - V_{\rm CNP} = -36$ V, where a low-pass filter with a cutoff frequency of 2.6 Hz has been applied. Black curve represents the noise background. Hall noise, measured simultaneously, is plotted in (b). (c) Noise magnitudes and their corresponding current dependence at different back gate voltages are plotted in log-log scale for the longitudinal and Hall voltage PSDs. All straight lines have a slope of 2, indicating a quadratic current dependence. Data in this figure are from sample B, measured at $T = 180$ K.

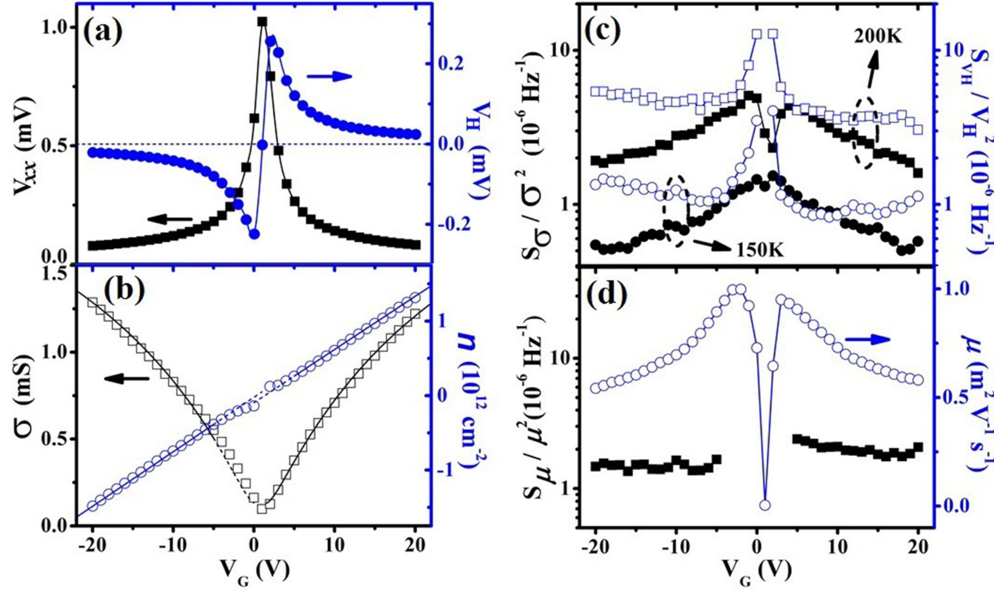

FIG. 4. (Color online) (a) Longitudinal (black squares) and Hall voltages (blue circles) plotted as a function of gate voltage. (b) Conductance (black squares) and carrier density (blue circles) values are derived from (a). Separate fittings for electron and hole lead to the same slope but different V_{CNP} (0.3 V for hole and 1.33 V for electron, which is ascribed to the hysteresis effect). (c) Normalized longitudinal noise PSD (solid black squares) and Hall noise PSD (open blue symbols) plotted as functions of gate voltage for $T = 150$ and 200 K. Away from the CNP, the Hall noise is shown to be larger than that for the longitudinal noise. (d) Mobility noise (solid black squares) displays no strong relation with gate voltage. Derived values of time-averaged mobility are plotted in open symbols, with the scale shown on the right. Data in this figure are from sample A at $T = 150$ K.

C. Comparison between the longitudinal noise and Hall noise

In Figs. 4(a) and 4(b) we show the experimental results of time-averaged data at 150 K. Similar behavior is found at $T = 200$ and 250 K. Time-averaged values of V_{xx} (black squares) and V_H (blue circles) are shown in Fig. 4(a) as a function of V_G. Derived σ (black open squares) and n (blue open circles) are plotted in Fig. 4(b). Best fittings (blue lines) for electrons (positive gate voltage) and holes (negative gate voltage) are shown to display the same slope, an indication that there is minimal mixture between V_{xx} and V_H.

In Figs. 4(c) and 4(d), we present the normalized PSDs of longitudinal noise (conductance noise), Hall noise, and mobility noise, respectively. Normalized PSDs of longitudinal noise (filled symbols) and Hall noise (open symbols) are plotted for $T = 150$ and 200 K as shown in Fig. 4(c). In Fig. 4(d) the time-averaged value of mobility is plotted as blue open circles, whereas its noise PSD is shown as black solid symbols. For longitudinal noise, the normalized PSDs show the "M" type characteristic, i.e., there is a dip at the CNP. The normalized PSD of longitudinal noise is a measurement of conductance (resistance) fluctuations. One can easily show, with a few algebraic steps, that the longitudinal fluctuations may be expressed as

$$\langle(\delta\sigma/\sigma)^2\rangle = \langle(\delta n/n)^2\rangle + \langle(\delta\mu/\mu)^2\rangle + 2\langle(\delta n/n)(\delta\mu/\mu)\rangle. \quad (1)$$

Hall voltage is a little complicated near the CNP for there are both electrons and holes, owing to the existence of the electron-hole puddles in graphene. If we focus on the region away from the CNP, then the Hall voltage is inversely proportional to the carrier density, i.e., $V_H = IB/ne$. In this region, the Hall noise PSD S_{VH} can be derived as the fluctuations of carrier densities:

$$S_{VH}/V_H^2 \propto \langle(\delta n/n)^2\rangle. \quad (2)$$

For $|V_G - V_{\mathrm{CNP}}| > 4$ V the normalized Hall noise PSD, which is equivalent to the carrier density noise PSD, is seen to be larger than the normalized longitudinal noise PSD. Note that in order to compare the longitudinal noise PSD and the Hall noise PSD, one needs to take into account the sample geometry [31,38,39], i.e., the distance between the voltage probes. The above conclusion is valid even after taking into account such geometric considerations, i.e., there is significant overlap in the spatial regions probed by the longitudinal and Hall voltages. The comparison between Hall noise and longitudinal noise magnitude indicates that the correlation term in Eq. (1) is negative; thus there is a negative correlation between carrier density and mobility fluctuations.

It should also be noted that from Fig. 4(c), S_n/n^2 is nearly constant as a function of V_G for $|V_G - V_D| > 4$ V. This is not completely trivial since in noise analysis the formula $S_R/R^2 = [(dR/dn)^2/R^2]S_n$ is often used, with the implicit understanding that S_n does not exhibit a strong gate-voltage dependence. However, our data show that S_n/n^2, rather than S_n, is nearly a constant.

IV. PHYSICAL INTERPRETATION

In this section we use the Boltzmann transport theory to quantitatively explain our experimental data. Within the Boltzmann transport theory and through the consideration of short-range scatterings, the time-averaged value of mobility is observed to decrease with increasing time-averaged value of carrier density. However, the instantaneous data of carrier

density and mobility are found to deviate from the time-averaged behavior, i.e., to explain the fluctuations one must go beyond the Boltzmann transport theory. We propose a simple one-parameter model to describe the observed behavior. In our model, the trapped charge carriers would neutralize the charged impurities, thereby enhancing the instantaneous mobility. Below we first determine the parameters of the transport theory by fitting the time-averaged values (μ_0,n_0), and then apply our model to the instantaneous data (μ,n).

A. Boltzmann transport theory

The time-averaged values of (μ_0,n_0) are plotted in the inset of Fig. 5. It is clearly seen that μ_0 decreases with increasing n_0, which can be well fitted by the Boltzmann transport theory. The Boltzmann transport gives the following conductance expression:

$$\sigma = \frac{e^2}{2} g(\varepsilon_F) v_F^2 \tau(\varepsilon_F), \tag{3}$$

where $g(\varepsilon_F)$ is the density of states at the Fermi energy, v_F is the Fermi velocity, and $\tau(\varepsilon_F)$ is the relaxation time at the Fermi level. In graphene, both long-range and short-range impurities exist. The relaxation time for the short-range scatterings is given by [40,41]

$$\tau_s = \frac{4(\hbar v_F)^2}{E_F} \frac{\hbar}{n_s V_s^2}, \tag{4}$$

where n_s is the density of short-range scattering impurities and V_s denotes their scattering strength. For long-range scatterings, which are caused by the charged impurities with the Coulomb potential, the corresponding long-range relaxation time is

$$\tau_l = \frac{4\hbar k}{\pi v_F} \frac{1}{n_i F(r_s)}, \tag{5}$$

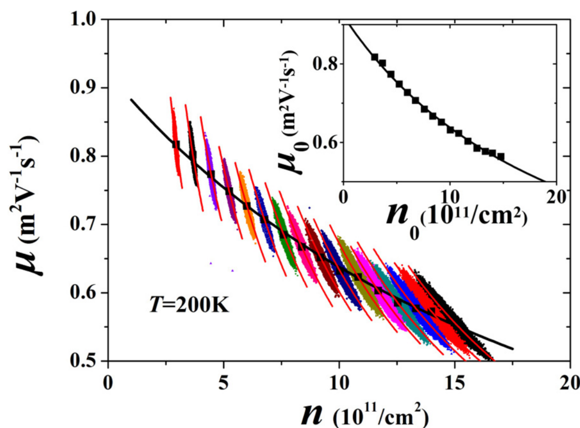

FIG. 5. (Color online) Instantaneous Hall mobility μ plotted as a function of the instantaneous carrier density n, for data taken at 200 K. The time-averaged mean values of (μ,n) are shown in the inset, where the solid square dots are the experimental data and the black curve represents the best fit. At each gate voltage (in intervals of 1 V, varying from 5 to 19 V for the electrons), the fluctuating pairs of (μ,n) are plotted in different colors. The thin red curves are fitting results from our trapping and detrapping model.

where $F(r_s) \equiv r_s^2 \int \frac{\sin^2\theta}{(\sin(\theta/2)+2r_s)^2} d\theta$ and n_i is the average density of long-range scattering impurities. The parameter r_s is the (dimensionless) Coulomb interaction parameter, defined as the ratio between the average Coulomb potential energy to the kinetic energy. For graphene on a SiO_2 substrate, $r_s \approx 0.9$.

When both the long-range and short-range scatterings are taken into account, the time-averaged mobility can be written as

$$\mu_0 = \frac{8e}{h} \frac{1}{(n_0/A) + 0.39 n_i}, \tag{6a}$$

where A is a dimensionless short-range scattering parameter $A \equiv \frac{(\hbar v_F)^2}{n_s V_s^2}$, and n_0 refers to the time-averaged carrier density under a given gate voltage. It is obvious that the first term in the denominator of Eq. (6a), which comes from the short-range scattering, causes a dreceasing μ_0 with increasing n_0. The formula can be used to fit the time-averaged data (μ_0,n_0) for sample A with the parameter values $A = 9.8 \pm 0.3$, $n_i = (4.64 \pm 0.05) \times 10^{11}$ cm^{-2} at $T = 150$ K; $A = 10.7 \pm 0.2$, $n_i = (5.24 \pm 0.03) \times 10^{11}$ cm^{-2} at $T = 200$ K (shown as the black curve in the inset of Fig. 5); and $A = 10.8 \pm 0.2$, $n_i = (5.52 \pm 0.03) \times 10^{11}$ cm^{-2} at $T = 250$ K. It should be noted that the Coulomb impurity density tends to increase with increasing temperature. That suggests a thermal activation process for the charged impurities, based on the detrapping of the charge carriers with increasing temperature.

B. Correlation between the carrier density and mobility fluctuations

In Fig. 5 the *mean values* of μ and n from sample A at $T = 200$ K are shown as the black curve. At each gate voltage, the *instantaneous mobility* is plotted, in a color other than black, as a function of its corresponding *instantaneous carrier density*. It is seen that the fluctuating pairs (μ,n) are not distributed along the same curve governing their mean values. The fluctuating pairs clearly display a steeper (negative) slope. That is, if we take the relation between the mean values (black curve) as the baseline, then a *decrease* in the fluctuating n would correspond with a positive *increase* in mobility that is in excess of the baseline case. This is a clear indication for the existence of negative correlation. In other words, the instantaneous mobility μ cannot be described as a function of carrier density n only; thus Eq. (6a) is not able to describe the instantaneous (μ,n) data.

We propose a model to describe this negative correlation between these two fluctuations as shown in Fig. 6. In this cartoon picture, there are charged impurity (Coulomb) centers in the system, and the transport carriers might be trapped by this type of Coulomb centers, resulting in an instantaneous decrease of transport carriers. Thus, even at the slightly different gate voltages, it is still possible to have the same number of carriers in the transport channel at a given instant. This is just what we have observed in Fig. 5, where the instantaneous data of (μ,n) obtained from different gate voltages can share the same carrier density. When the transport carriers are trapped, not only the carrier density decreases but also the charged impurities are neutralized, thereby enhancing the mobility. In Boltzmann transport theory, the charged impurity density n_i is a constant, but now it should be regarded

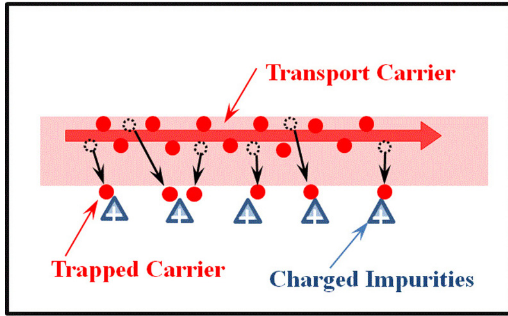

FIG. 6. (Color online) Cartoon picture for the trapping and detrapping model. For different gate voltages, the trapping and detrapping of carriers not only can vary the net charge carrier density at any moment, but also would "neutralize" the charged impurities, thereby leading to altered (instantaneous) mobility.

as a function dependent on the trapped carriers density δn. Hence we assume that when n fluctuates, n_i can also fluctuate as a function of $(n-n_0)/n_0$, i.e., $n_i \equiv n_i(\frac{n-n_0}{n_0})$, where n is the instantaneous carrier density and n_0 is the time-averaged value. To further simplify this model, we apply the linear expansion to $n_i \simeq n_i(1-\alpha(n-n_0)/n_0)$, where α is the Taylor expansion coefficient, treated here as a phenomenological parameter. On the basis of Eq. (6a), for the *instantaneous* mobility μ, we rewrite Eq. (6a) as

$$\mu = \frac{8e}{h}\frac{1}{(n/A)+0.39n_i[1-\alpha(n-n_0)/n_0]}, \qquad (6b)$$

where the parameter α is introduced to quantify the effect of the fluctuating n on the density of Coulomb scattering centers n_i. For a negative α, the plausible physics underlying Eq. (6b) can be stated as follows. When there is a transient deficit of charge carrier density as compared to n_0, that deficit may be regarded as effectively neutralizing some of the Coulomb scattering centers with the opposite charge, thereby enhancing the mobility. However, this must be a transient event; i.e., detrapping would occur for any particular trapped charge carrier. The time duration in which the charge carrier is trapped by the oppositely charged Coulomb impurity center can vary with temperature. With increasing temperature, the time duration a carrier remains trapped can decrease, implying that on average there can be more "net" n_i. With such trapping and detrapping, a negative α implies negative correlation between the charge carrier density and mobility fluctuations. Equation (6b) can be used to fit the instantaneous (μ,n). The best fit is shown in Fig. 6, with $\alpha=-1$.

Equation (6b) can be expressed alternatively as

$$\mu = \frac{8e}{h}\frac{1}{(n/A')+0.39n_i^*}, \qquad (7a)$$

where $1/A' = (1/A) - 0.39\alpha(n_i/n_0)$ and $n_i^* = (1+\alpha)n_i$. With the fitting result $\alpha=-1$, we can find that $n_i^*=0$. If we define a new parameter

$$\tilde{n} \equiv n/A' = n[A^{-1}+0.39(n_i/n_0)], \qquad (7b)$$

then Eq. (7a) can be rewritten as

$$\mu = \frac{8e}{h}\frac{1}{n[A^{-1}+0.39(n_i/n_0)]} = \frac{8e}{h}\frac{1}{\tilde{n}}. \qquad (7c)$$

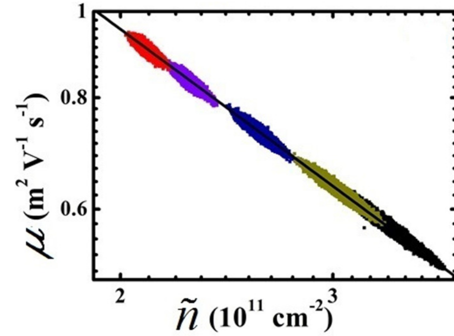

FIG. 7. (Color online) A log-log plot of fluctuating pair $(\mu,\tilde{n})$ with data collected at gate voltages of 5 V (red), 7 V (crimson), 10 V (dark blue), 15 V (green), and 20 V (black). An excellent linear relation is obtained, with all the data collapsing on a straight line as predicted by Eq. (7c). Data in this figure are from sample A measured at $T = 150$ K.

In Fig. 7 we plot the fluctuating values of the pair $(\mu,\tilde{n})$ collected at different gate voltages; it is seen that all the instantaneous data pairs $(\mu,\tilde{n})$ collapse onto the same straight line. Excellent agreement is obtained with the prediction as expressed by Eq. (7c) in which $A = 9.8$ (corresponding to $\rho_s = 330\ \Omega$ at 150 K), $n_i = 4.6\times10^{11}$ cm^{-2}, and n_0 obtained at each different gate voltage. The fact that $\alpha=-1$ can explain the data so well implies that all of $\delta n = n - n_0$ participates in the trapping and detrapping process, involving the Coulomb scatterers. The net result for the instantaneous mobility can be modeled as arising from a temporal modulation of the density of long-range scatterers through the fluctuating n.

C. Cross correlation between longitudinal and Hall noise

As the longitudinal and Hall voltages are collected simultaneously, the correlation between these two signals can be analyzed. The experimental results indicate that there is no correlation between these two fluctuations as shown in Fig. 8. For both samples A and B, the correlation coefficient is plotted as a function of back gate voltage in Figs. 8(a) and 8(b). The correlation coefficient is almost 0 for both samples. For sample B, the real-time data of longitudinal and Hall voltages are shown in the inset of Fig. 8(b). No obvious correlation can be seen in the time domain. The fact that the longitudinal and Hall voltage fluctuations have no correlation is actually surprising at first sight. As discussed previously, the Hall noise arises from the carrier density fluctuations only. For the longitudinal noise, there are two corresponding fluctuating sources, i.e., mobility and carrier density. Since the carrier density appears in both, the Hall noise and longitudinal noise should be correlated.

To consistently explain our results, we assume that the *fluctuations of mobility consist of two components*: one associated with fluctuations in charge carrier density, denoted by $\delta\mu^{(1)}$, and the other associated with the changing configuration of scattering centers, denoted by $\delta\mu^{(2)}$. Since $\delta\mu^{(2)}$ is independent of electron trapping and detrapping, there is no correlation between this part and the fluctuating charge carrier density δn. Thus we can write

$$\begin{aligned} -\delta V_{xx}/V_{xx} &= (\delta n/n) + (\delta\mu/\mu) \\ &= [(\delta n/n) + (\delta\mu^{(1)}/\mu)] + (\delta\mu^{(2)}/\mu). \end{aligned} \qquad (8a)$$

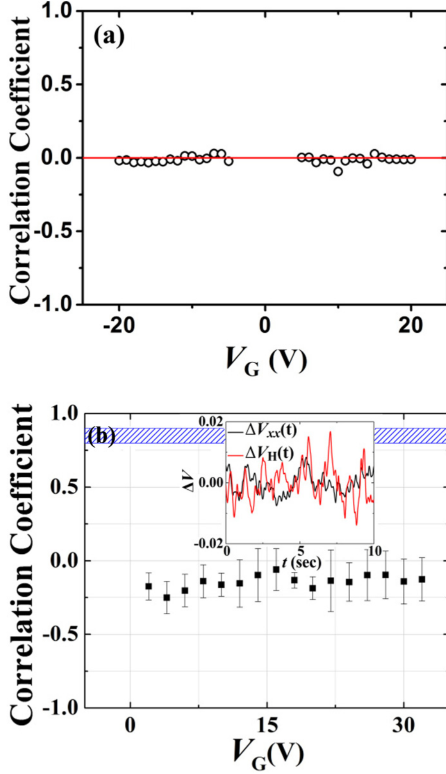

FIG. 8. (Color online) (a) Correlation coefficient (from sample A) as a function of gate voltages obtained from ten sets of voltage signals with each set lasting 125 s, with a sampling rate of 512 Hz. Data were taken at $T = 150$ K. (b) Correlation coefficient (from sample B) plotted as a function of gate voltages. Blue shaded region represents the range of correlation coefficient measured in semiconductors on sapphire (SOS) systems Ref. [28]. The inset image is the fluctuating longitudinal voltage (black) and Hall voltage (red) from sample B are shown in time domain. The fluctuations for longitudinal and Hall voltages are defined as $\Delta V_{xx(H)}(t) \equiv [V_{xx(H)}(t) - V^{\text{average}}_{xx(H)}]/V^{\text{average}}_{xx(H)}$. Data were taken at $T = 180$ K.

If $\delta\mu^{(1)}/\mu$ is negatively correlated with $\delta n/n$, then the first term on the right-hand side of Eq. (8a), $[(\delta n/n) + (\delta\mu^{(1)}/\mu)]$, denoted as $\delta\sigma^{(1)}/\sigma$, has a zero value and does not contribute to the longitudinal noise (see below). Hence we can effectively rewrite Eq. (8a) as

$$-\delta V_{xx}/V_{xx} = \delta\mu^{(2)}/\mu. \tag{8b}$$

Since δn and $\delta\mu^{(2)}$ are independent of each other, hence $\delta V_{xx}(t)$ and $\delta V_H(t)$ should have no correlation as shown in Fig. 8(b). Furthermore, from our measurements the normalized noise PSD of δn is larger than that of $\delta\mu^{(2)}$.

Equation (7a) implies some simple relationships between the normalized PSDs of different physical quantities. For the Hall noise, we have $S_{VH}/V_H^2 = S_n/n^2$. By differentiating Eq. (7a) we obtain

$$\frac{\delta\mu^{(1)}}{\delta n} = -\frac{8e}{h}\frac{1}{A'[(n/A') + 0.39n_i^*]^2}. \tag{9}$$

Hence it follows that

$$\frac{S_\mu^{(1)}/\mu^2}{S_n/n^2} = \frac{(\delta\mu^{(1)})^2/\mu^2}{\delta n^2/n^2} = \frac{(n/A')^2}{[(n/A') + 0.39n_i^*]^2}. \tag{10}$$

For $n_i^* = 0$, we have $S_\mu^{(1)}/\mu^2 = S_n/n^2$, i.e., the component of mobility that is negatively correlated with the charge carrier density has the same normalized noise PSD as that of n. Furthermore, from $\delta\sigma/\sigma = (\delta\sigma^{(1)}/\sigma) + (\delta\sigma^{(2)}/\sigma) = [(\delta n/n) + (\delta\mu^{(1)}/\mu)] + (\delta\mu^{(2)}/\mu)$, we obtain

$$\frac{S_\sigma^{(1)}/\sigma^2}{S_n/n^2} = \frac{(0.39n_i^*)^2}{[(n/A') + 0.39n_i^*]^2}. \tag{11}$$

That is, the normalized noise PSD for $\delta\sigma^{(1)}/\sigma$ is zero when $\alpha = -1$ so that $n_i^* = 0$. From Eqs. (10) and (11) we can also deduce the identity

$$\sqrt{S_\sigma^{(1)}/\sigma^2} = \sqrt{S_n/n^2} - \sqrt{S_\mu^{(1)}/\mu^2}, \tag{12}$$

which explicitly expresses the negative correlation between the fluctuations of charge carrier density and one component $(\delta\mu^{(1)}/\mu)$ of the mobility. With $\alpha = -1$, Eq. (12) yields the same conclusion as previously stated, i.e., $S_\sigma^{(1)}/\sigma^2 = 0$. Therefore the main component of fluctuations in the longitudinal conductance (voltage) arises from $\delta\mu^{(2)}$, i.e.,

$$S_\sigma/\sigma^2 = S_\sigma^{(2)}/\sigma^2 = S_\mu^{(2)}/\mu^2, \tag{13}$$

and $S_n/n^2 > S_\mu^{(2)}/\mu^2$ from our data [Fig. 4(c)]. The result as stated by Eq. (13) can also explain the reason why mobility fluctuations dominate longitudinal resistance fluctuations as reported in the literature [9].

D. Spatial and temporal correlations

The *simultaneous* measurement is crucial in our experimental measurements. As mobility is expressed as a function of both longitudinal and Hall voltage, it is only when both voltages are measured simultaneously that can we define a meaningful mobility. The $1/f$ characteristic of our noise data is robust within a certain frequency range, i.e., from 0.01 to 1 Hz, which corresponds to the correlation function from 1 to 100 s in the time domain. Our *simultaneous* measurement is achieved by the same trigger signal from one lock-in, which makes the time error between two lock-in signals less than 1 μs. Comparing the time scale in the correlation function, our signals collected by two lock-ins are indeed at the same time.

Another aspect about the correlation is that the Hall and longitudinal measurements must probe the same or overlapping spatial regions of the sample. If different regions are measured for longitudinal and Hall noise, then the mobility we derived from two voltages is trivially ill defined. We have indeed measured the cross correlation between different voltages in sample A. The cross correlation coefficient between two Hall voltages turns out to be zero, while the cross correlation between two longitudinal voltages is larger than 0.9. We can attribute the absence of correlation between the two Hall voltages to probing two spatially distinct regions, while the longitudinal voltages are probing the same area, leading to the correlation coefficient being almost 1.

If the Hall voltages and longitudinal voltages are measured simultaneously, the cross correlation coefficient should be nonzero. As shown in Fig. 1(a), we note that there is an overlapping area probed by both V_{xx} and V_H. This overlapping area between Hall and longitudinal voltage probes is 0.4 μm × 0.8 μm, and the area accounting for the longitudinal

noise is 1.6 μm $\times$ 0.8 μm. Hence the ratio is about 25%. If the noises arise from the same source (carrier density fluctuations), the correlation coefficient should be $\sim$0.25. However, the measurement results are more than one order of magnitude smaller [see Fig. 8(a)], exhibiting the absence of cross correlation.

For sample B with a square (cross-bar) geometry, the Hall and longitudinal voltages probe the same area. Again, we observed that the correlation coefficient between longitudinal and Hall fluctuations is small as shown in Fig. 8(b). The real-time data of longitudinal and Hall voltages are plotted as a function of time, and no correlation can be observed, as shown in the inset picture.

V. CONCLUDING REMARKS

In conclusion, we have used simultaneous Hall and longitudinal measurements to directly deduce charge carrier density and mobility fluctuations. The relation governing the instantaneous carrier density and mobility does not follow the relation between their (time-averaged) mean values, and implies negative correlation between one component of the mobility fluctuations and carrier density fluctuations. Being dominated by the remaining component of the mobility fluctuations, the longitudinal noise displays no correlation to the Hall noise, and has a normalized PSD that is smaller than that of the Hall noise.

The temperature dependence observed in our (deduced) values of n_i suggests that at low temperatures, the trapped carriers can be frozen at the Coulomb impurity centers with little chance to be released. Hence in such case this component of the noise would tend towards a small magnitude. The carrier density may then have a dependence on the bias voltage, owing to the release of the carriers from the Coulomb trap centers through the bias field, with the attendant mobility displaying a correlation with the carrier density variation. Such implication remains to be verified.

ACKNOWLEDGMENTS

We wish to acknowledge the support by SRFI11/SC02 and the Research Grants Council of Hong Kong, Grant No. HKUST9/CRF/08. J.J.L. was supported by the Taiwan National Science Council through Grant No. NSC 102-2120-M-009-003.

[1] M. B. Weissman, Rev. Mod. Phys. **60**, 537 (1988).
[2] F. Schwierz, Nat. Nanotechnol. **5**, 487 (2010).
[3] S. Pisana, P. M. Braganca, E. E. Marinero, and B. A. Gurney, Nano Lett. **10**, 341 (2010).
[4] J. M. Lu, H. J. Zhang, W. Shi, Z. Wang, Y. Zheng, T. Zhang, N. Wang, Z. K. Tang, and P. Sheng, Nano Lett. **11**, 2973 (2011).
[5] H. Xu, Z. Zhang, R. Shi, H. Liu, Z. Wang, S. Wang, and L.-M. Peng, Sci. Rep. **3**, 1207 (2013).
[6] F. Schedin, A. K. Geim, S. V. Morozov, E. W. Hill, P. Blake, M. I. Katsnelson, and K. S. Novoselov, Nat. Mater. **6**, 652 (2007).
[7] S. Rumyantsev, G. X. Liu, M. S. Shur, R. A. Potyrailo, and A. A. Balandin, Nano Lett. **12**, 2294 (2012).
[8] M. S. Artiles, C. S. Rout, and T. S. Fisher, Adv. Drug Delivery Rev. **63**, 1352 (2011).
[9] A. N. Pal, S. Ghatak, V. Kochat, E. S. Sneha, A. Sampathkumar, S. Raghavan, and A. Ghosh, ACS Nano **5**, 2075 (2011).
[10] A. A. Kaverzin, A. S. Mayorov, A. Shytov, and D. W. Horsell, Phys. Rev. B **85**, 075435 (2012).
[11] Y. Zhang, E. E. Mendez, and X. Du, ACS Nano **5**, 8124 (2011).
[12] Z. Chen, Y.-M. Lin, M. J. Rooks, and P. Avouris, Physica E (Amsterdam, Neth.) **40**, 228 (2007).
[13] J. T. Robinson, F. K. Perkins, E. S. Snow, Z. Q. Wei, and P. E. Sheehan, Nano Lett. **8**, 3137 (2008).
[14] Y. M. Lin and P. Avouris, Nano Lett. **8**, 2119 (2008).
[15] G. Liu, W. Stillman, S. Rumyantsev, Q. Shao, M. Shur, and A. A. Balandin, Appl. Phys. Lett. **95**, 033103 (2009).
[16] A. N. Pal and A. Ghosh, Phys. Rev. Lett. **102**, 126805 (2009).
[17] A. N. Pal and A. Ghosh, Appl. Phys. Lett. **95**, 082105 (2009).
[18] Q. H. Shao, G. X. Liu, D. Teweldebrhan, A. A. Balandin, S. Runryantsev, M. S. Shur, and D. Yan, IEEE Electron Device Lett. **30**, 288 (2009).
[19] Z. G. Cheng, Q. Li, Z. J. Li, Q. Y. Zhou, and Y. Fang, Nano Lett. **10**, 1864 (2010).
[20] I. Heller, S. Chatoor, J. Mannik, M. A. Zevenbergen, J. B. Oostinga, A. F. Morpurgo, C. Dekker, and S. G. Lemay, Nano Lett. **10**, 1563 (2010).
[21] S. A. Imam, S. Sabri, and T. Szkopek, Micro Nano Lett. **5**, 37 (2010).
[22] S. Rumyantsev, G. Liu, W. Stillman, M. Shur, and A. A. Balandin, J. Phys.: Condens. Matter. **22**, 395302 (2010).
[23] G. Xu, C. M. Torres, Jr., Y. Zhang, F. Liu, E. B. Song, M. Wang, Y. Zhou, C. Zeng, and K. L. Wang, Nano Lett. **10**, 3312 (2010).
[24] S. L. Rumyantsev, G. Liu, M. S. Shur, and A. A. Balandin, Appl. Phys. Lett. **98**, 222107 (2011).
[25] B. Grandchamp, S. Fregonese, C. Majek, C. Hainaut, C. Maneux, N. Meng, H. Happy, and T. Zimmer, IEEE Trans. Electron Devices **59**, 516 (2012).
[26] S. K. Lee, C. G. Kang, Y. G. Lee, C. Cho, E. Park, H. J. Chung, S. Seo, H.-D. Lee, and B. H. Lee, Carbon **50**, 4046 (2012).
[27] A. A. Balandin, Nat. Nanotechnol. **8**, 549 (2013).
[28] R. D. Black, P. J. Restle, and M. B. Weissman, Phys. Rev. B **28**, 1935 (1983).
[29] J. Brophy, Phys. Rev. **106**, 675 (1957).
[30] Ç. Kurdak, C. J. Chen, D. C. Tsui, S. Parihar, S. Lyon, and G. W. Weimann, Phys. Rev. B **56**, 9813 (1997).
[31] I. S. Bakshi, M. Z. Kodalashvili, E. A. Salkov, and B. I. Khizhnyak, Sov. Phys. Semicond. **22**, 1377 (1988).
[32] R. Jayaraman and C. G. Sodini, IEEE Trans. Electron Devices **36**, 1773 (1989).
[33] M. v. Haartman, Royal Institute of Technology (KTH), Doctoral thesis, 2006.
[34] I. I. Boiko, arXiv:1011.4204 [cond-mat.mes-hall].
[35] A. Venugopal, J. Chan, X. Li, C. W. Magnuson, W. P. Kirk, L. Colombo, R. S. Ruoff, and E. M. Vogel, J. Appl. Phys. **109**, 104511 (2011).

[36] H. Zhang, J. Lu, W. Shi, Z. Wang, T. Zhang, M. Sun, Y. Zheng, Q. Chen, N. Wang, J.-J. Lin, and P. Sheng, Phys. Rev. Lett. **110**, 066805 (2013).
[37] S. Cho and M. S. Fuhrer, Phys. Rev. B **77**, 081402(R) (2008).
[38] L. K. J. Vandamme and W. M. G. Vanbokhoven, Appl. Phys. **14**, 205 (1977).
[39] L. K. J. Vandamme and L. P. J. Kamp, J. Appl. Phys. **50**, 340 (1979).
[40] S. Adam, E. H. Hwang, V. M. Galitski, and S. Das Sarma, Proc. Natl. Acad. Sci. USA **104**, 18392 (2007).
[41] S. Das Sarma, S. Adam, E. H. Hwang, and E. Rossi, Rev. Mod. Phys. **83**, 407 (2011).